

# Nuclear Envelope Rupture Is Enhanced by Loss of p53 or Rb

Zhe Yang, John Maciejowski, and Titia de Lange



## Abstract

The mammalian nuclear envelope (NE) forms a stable physical barrier between the nucleus and the cytoplasm, normally breaking down only during mitosis. However, spontaneous transient NE rupture in interphase can occur when NE integrity is compromised, such as when the nucleus experiences mechanical stress. For instance, deficiencies in the nuclear lamins and their associated proteins can cause NE rupture that is promoted by forces exerted by actin filaments. NE rupture can allow cytoplasmic nucleases to access chromatin, potentially compromising genome integrity. Importantly, spontaneous NE rupture was noted in several human cancer cell lines, but the cause of this defect is not known. Here, we investigated the mechanistic contributions of two major tumor suppressors, p53 (TP53) and Rb (RB1), to the

repression of NE rupture. NE rupture was induced in normal human epithelial RPE-1 cells upon impairment of either Rb or p53 achieved by shRNA knockdown and CRISPR/Cas9 gene editing. NE rupture did not involve diminished expression of NE components or greater cell motility. However, cells that underwent NE rupture displayed a larger nuclear projection area. In conclusion, the data indicate that NE rupture in cancer cells is likely due to loss of either the Rb or the p53 pathway.

**Implications:** These findings imply that tumor suppression by Rb and p53 includes the ability to prevent NE rupture, thereby protecting against genome alterations. *Mol Cancer Res*; 15(11); 1579–86. ©2017 AACR.

## Introduction

The nuclear envelope (NE) is composed of the inner nuclear membrane (INM), to which the nuclear lamina is attached, and the outer nuclear membrane (ONM), which is contiguous with the endoplasmic reticulum (ER). The NE prevents macromolecules from diffusing into and out of the nucleus, thus maintaining the separation between the cytoplasm and the nucleoplasm and allowing the nuclear pore complexes (NPCs) to regulate the trafficking of macromolecules (1). In prophase, NE fragmentation and dissolution allow mitotic chromosomes to attach to the microtubule spindle. In telophase, the NE reforms, surrounding the decondensing chromatin and reestablishing the physical barrier between the nucleus and the cytoplasm (2).

Although NE breakdown was thought to occur only during mitosis, it has recently become clear that NE rupture can occur transiently during interphase under specific conditions (3). Cells derived from patients with laminopathy, a genetic disorder caused by mutations in lamin or lamin-associated proteins, show transient NE rupture in interphase (4). In addition, during parvovirus infection, the NE and lamina break down, allowing viral particles to enter the nucleus (5). Although the NE is usually resealed rapidly, NE rupture can have detrimental effects due to mislocalization of cytoplasmic proteins and organelles (4, 6).

Recent studies have pointed to mechanical stress as a major source of NE rupture in cells with lamin deficiencies. Contractile actin bundles that increase nuclear pressure contribute to NE rupture and chromatin herniation (7). This finding is consistent with the role of the linker of nucleoskeleton and cytoskeleton complex (LINC complex, composed of SUN and Nesprin proteins) in exacerbating NE rupture in cells with deficiencies in the nuclear lamina (8) and with the finding that increased stiffness of the substratum promotes NE rupture in cells with Lamin A mutations (9). Mechanical stress is also implicated in NE rupture in primary cells that migrate through tight spaces (10, 11) and NE rupture can be induced by simply flattening HeLa nuclei mechanically (12). Furthermore, mechanical stress exerted by pulling forces on nuclei could explain NE rupture resulting from the chromatin bridges formed by dicentric chromosomes (13). In this setting, NE rupture allows a cytoplasmic nuclease, TREX1, to fragment the chromatin in the bridges, giving rise to chromothripsis (13). This DNA fragmentation exemplifies the risk of genome alterations associated with NE rupture.

Interestingly, a permanent form of NE rupture has been noted in micronuclei (14). This lack of NE integrity is thought to promote fragmentation of the resident chromatin and has been implicated in the chromothripsis of micronuclear chromosomes (15, 16).

Cells are protected against deleterious consequences of NE rupture by the ESCRT-III complex, which can rapidly reestablish NE integrity (10, 11). In addition, perinuclear actin nucleated by Formin-2 (FMN2) protects nuclei from NE rupture and ensuing DNA damage during cell migration (17). Interestingly, FMN2 is upregulated in melanoma, potentially allowing cells to survive extravasation during the development of metastatic disease.

Importantly, several human cancer cell lines (HeLa, U2OS, and SJSa), which have no known lamin deficiency, show spontaneous NE rupture in the absence of extraneous mechanical stress (6). The reason for this propensity of cancer cell lines for NE rupture is not

Laboratory for Cell Biology and Genetics, The Rockefeller University, New York, New York.

**Note:** Supplementary data for this article are available at Molecular Cancer Research Online (<http://mcr.aacrjournals.org/>).

**Corresponding Author:** Titia de Lange, Laboratory of Cell Biology and Genetics, Rockefeller University, Box 159, 1230 York Avenue, New York, NY 10065-6399. Phone: 212-327-8146; Fax: 212-327-7147; E-mail: [delange@rockefeller.edu](mailto:delange@rockefeller.edu)

**doi:** 10.1158/1541-7786.MCR-17-0084

©2017 American Association for Cancer Research.

Yang et al.

clear. We found that human RPE-1 cells show increased spontaneous NE rupture when both p21 and Rb are knocked down with shRNAs (13), potentially explaining NE rupture in cancer cell lines deficient in Rb or p53. Here, we test the individual contribution of p53 and Rb to this phenotype and report that loss of either p53 or Rb in RPE-1 cells enhances the frequency of NE rupture. Thus, loss of p53 or Rb function may be one of the causes of NE rupture in cancer cell lines.

## Materials and Methods

### Cell culture procedures and plasmids

hTERT RPE-1 cells were obtained from the ATCC and cultured in a 1:1 mixture of Dulbecco's Modified Eagle Medium (DMEM) and Ham's F-12 medium (DMEM/F12; Gibco). The cells have been tested to be free of *Mycoplasma* contamination by DAPI staining. Phoenix virus packaging cells were grown in DMEM. Media were supplemented with 10% fetal bovine serum (Gibco), 100 U/mL penicillin/streptomycin (Life Technologies), and 2.5 mmol/L L-glutamine (Life Technologies), 1 × Minimum NEAA (Gibco).

NLS-3xmTurquoise2 (13) was cloned into the retroviral pQCXIP vector. Retroviral constructs were transfected into Phoenix amphotropic packaging cells using calcium phosphate precipitation. Retroviral supernatants were filtered, mixed 1:1 with target cell media and supplemented with 4 µg/mL polybrene. Target cells were infected with retroviral supernatants four times at 12-hour intervals. Transduced cells were isolated by FACS.

pMKO.1-EV, pMKO.1-Rb shRNA, and pMKO.1-p53 shRNA#2 plasmids were purchased from Addgene (#8452, #10670, and #10672). Constructs were transfected into Phoenix amphotropic packaging cells, and target cells were infected as above. Infected cells were selected using puromycin (10 µg/mL).

Target sequences for CRISPR/Cas9-mediated gene knockouts were identified by ZiFit (<http://zifit.partners.org>): sgTP53: 5'-GGCAGCTACGTTTCCGTC-(PAM)-3', sgRB1: 5'-GGCCGCTGCTCT-(PAM)-3'. Target sequences were incorporated into a BbsI-linearized sgRNA-cloning vector that also contains mCherry-tagged Cas9 (Addgene # 64324). Plasmids were then transfected into target cells by nucleofection (Lonza apparatus). Cells (700,000) in electroporation buffer (freshly mixed 125 mmol/L

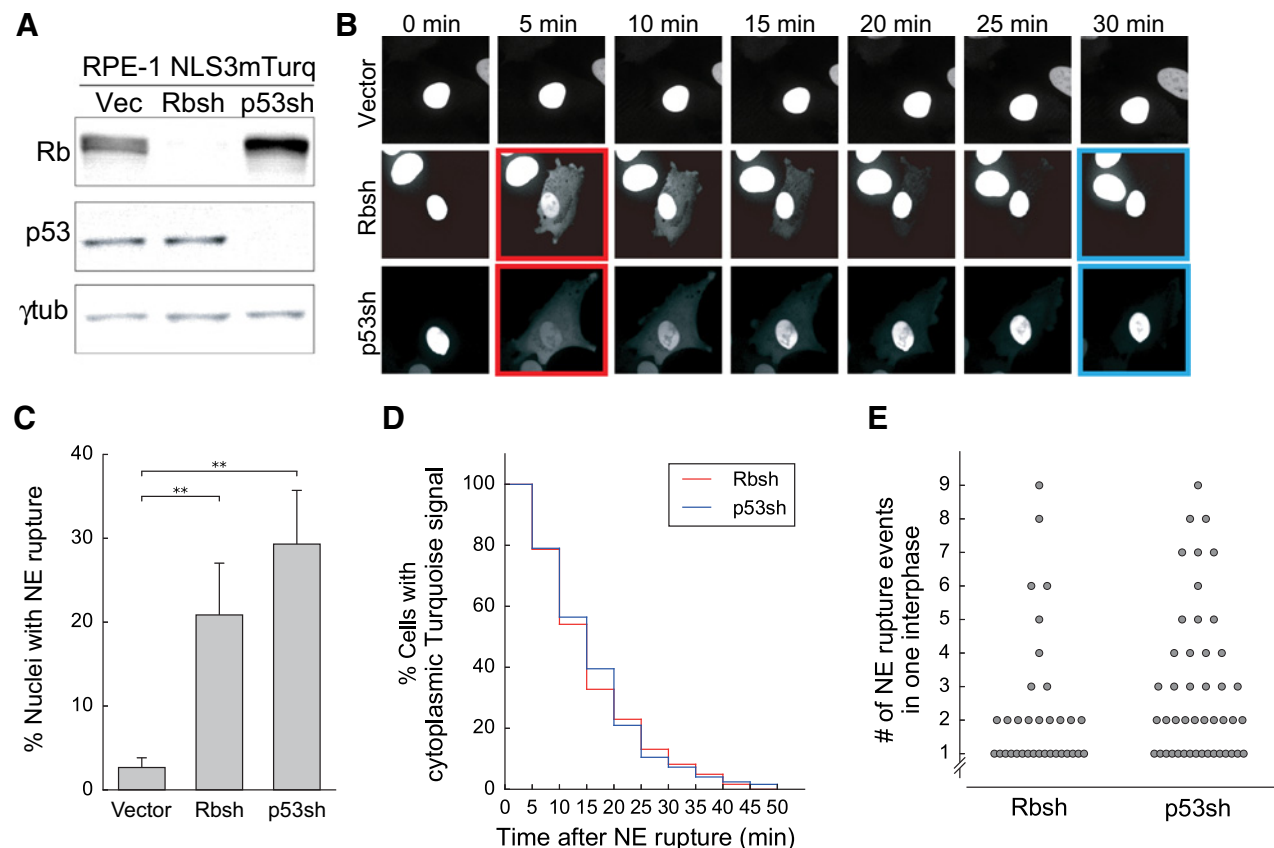


**Figure 1.**

Depletion of Rb or p53 with shRNAs in RPE-1 cells leads to NE rupture. **A**, Immunoblotting of Rb and p53 in RPE-1 cells infected with shRNAs with  $\gamma$ -tubulin as the loading control. **B**, Examples of transient NE rupture after Rb or p53 depletion in RPE-1 cells transfected with NLS3mTurq cells. The red squares indicate cells undergoing NE rupture, and the blue squares indicate cells with NLS3mTurq marker localization fully restored. **C**, Quantification of the percentage of nuclei with NE rupture. Error bars indicate SD and are derived from three separate experiments with at least 50 cells tracked in each experiment. \*\*,  $P < 0.01$  (Student *t* test). Fisher exact test,  $P < 0.0001$ . **D**, Timing of the full restoration of nuclear localization of NLS3mTurq in RPE-1 cells that had undergone NE rupture. Full restoration is marked when the cytoplasmic Turquoise signal was reduced to the original level before NE rupture. 60 NE rupture events were analyzed in each cell line.  $P = 0.98$  (Kolmogorov-Smirnov test). **E**, Quantification of the number of NE rupture events per cell per cell cycle. Only cells that underwent at least one NE rupture event are plotted.

$\text{Na}_2\text{HPO}_4$ , 12.5 mmol/L KCl, 55 mmol/L  $\text{MgCl}_2$  pH 7.75) were mixed with 10  $\mu\text{g}$  sgRNA plasmid, transferred to an electroporation cuvette (BTX), and electroporated with program T23 for RPE-1 cells. Cells were then allowed to recover for 48 hours before FACS sorting for mCherry positive cells. FACS-sorted cells were then collected in bulk and tested by Western blot for Rb or p53 knockout.

### Immunoblotting

For immunoblotting, cells were harvested by trypsinization and lysed in 1 $\times$  Laemmli buffer (50 mmol/L Tris, 10% glycerol, 2% SDS, 0.01% bromophenol blue, 2.5%  $\beta$ -mercaptoethanol) at  $10^7$  cells/mL. Lysates were denatured at  $100^\circ\text{C}$  and DNA was sheared with a 28 $^{1/2}$  gauge insulin needle. Lysate equivalent to  $10^5$  cells was resolved on 8% or 10% SDS/PAGE (Life Technologies) and transferred to nitrocellulose membranes. Membranes were blocked in 5% milk in TBS with 0.1% Tween-20 (TBS-T) and incubated with primary antibody overnight at  $4^\circ\text{C}$ , washed 3 times in TBS-T, and incubated for 1 hour at room temperature with horseradish-peroxidase-conjugated sheep anti-mouse or donkey anti-rabbit secondary antibodies. After three washes in TBS-T, membranes were rinsed in TBS, and proteins were developed using enhanced chemiluminescence (Amersham). Band intensity was quantified in Fiji.

The following primary antibodies were used: anti-Rb (mouse monoclonal, BD Pharmingen, #554136); anti-p53 (mouse monoclonal, Santa Cruz Biotechnology, sc-126); anti- $\gamma$  tubulin (mouse monoclonal, Abcam, ab11316); anti-Lamin A/C (mouse monoclonal, Santa Cruz Biotechnology, sc-7293); anti-Lamin B1 (rabbit polyclonal, Abcam, ab16048); anti-SUN1 (rabbit polyclonal, Abcam, ab74758); anti-SUN2 (rabbit polyclonal, Abcam,

ab87036); anti-LAP2 (rabbit polyclonal, Bethyl, A304-838A-T); anti-FMN2 (rabbit polyclonal, Abcam, ab72052); anti-CHMP2A (rabbit polyclonal, Proteintech, 10477-1-AP); anti-CHMP4B (rabbit polyclonal, Proteintech, 13681-1-AP).

### FACS

For cell-cycle analysis, cells were labeled with 10  $\mu\text{mol/L}$  BrdUrd for 30 minutes, fixed with cold 70% ethanol and stored overnight. BrdUrd-incorporated DNA was denatured with 2N HCl and 0.5% Triton X-100 for 30 minutes at room temperature. After neutralized with 0.1 mol/L  $\text{Na}_2\text{B}_4\text{O}_7 \cdot 10\text{H}_2\text{O}$  (pH 8.5), cells were incubated with fluorescein-isothiocyanate-conjugated anti-BrdUrd antibody (BD Biosciences) in PBS with 0.5% Tween 20 and 0.5% BSA for 30 minutes at room temperature. Cells were washed and stained with propidium iodide (2 mmol/L EDTA, 0.2 mg/mL RNase A, 10  $\mu\text{g/mL}$  propidium iodide in PBS). FACS was performed with an AccuriC6 (BD Biosciences), and data were analyzed by FlowJo software.

### Live-cell imaging

Cells (200,000) were plated onto 35-mm glass bottom dishes (MatTek) 24 hours before imaging. Live-cell imaging was performed using a CellVoyager CV1000 spinning disk confocal system (Yokogawa) equipped with 405-, 488-, and 561-nm lasers, and a Hamamatsu 512  $\times$  512 EMCCD camera. Pinhole size was 50  $\mu\text{m}$ . Images were acquired at the indicated intervals using a UPlanSApo 60x/1.3 silicone oil objective with the correction collar set to 0.17. The pixel size in the image was 0.27  $\mu\text{m}$ . A 480/40 emission filter was used for image acquisition for NLS-3xmTurquoise2. Sixteen z-stacks were collected at 1.33  $\mu\text{m}$  steps. Temperature was maintained at  $37^\circ\text{C}$  in a

**Figure 2.**

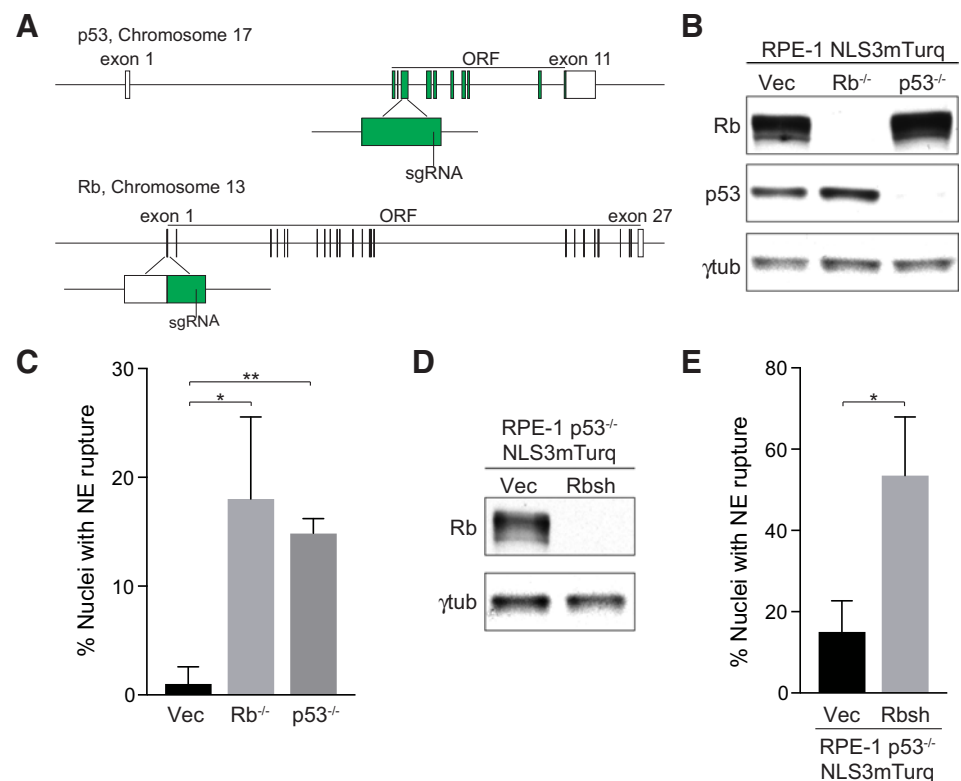
Rb or p53 knockout by CRISPR/Cas9 in RPE-1 cells leads to NE rupture.

**A**, Schematic of Rb and p53 gene editing with CRISPR/Cas9. The rectangles represent exons with green indicating coding sequences. The position of each sgRNA is depicted.

**B**, Verification of Rb and p53 knockout by Western blot. **C**, Quantification of the percentage of nuclei with NE rupture in Rb and p53 knockout cells. Error bars indicate SD and are derived from three separate experiments. \*,  $P < 0.05$ ; \*\*,  $P < 0.01$  (Student *t* test). Fisher's exact test,  $P < 0.0001$ .

**D**, Verification of Rb shRNA knockdown by western blot in the p53 knockout population shown in **B**.

**E**, Quantification of the percentage of nuclei with NE rupture in p53 knockout cells with or without Rb knockdown. Error bars indicate SD and are derived from three separate experiments. \*,  $P < 0.05$  (Student *t* test). Fisher exact test,  $P < 0.0001$ .



Yang et al.

temperature-controlled enclosure with CO<sub>2</sub> support. Maximum intensity projection of z-stacks and adjustment of brightness and contrast were performed using Fiji software. Image stitching was done with the Fiji plugin Grid/Collection stitching (18) with 20% tile overlap, linear blending, a 0.30 regression threshold, a 2.50 max/avg. displacement threshold, and a 3.50 absolute displacement threshold. Images were cropped and assembled into figures using Photoshop CS5.1 (Adobe). Cell tracking was done with Fiji plugin Manual Tracking (Fiji version 2.00-rc-54/1.51h). Nuclear surface area was measured by the manual tracing of nuclear borders in Fiji.

## Results

### Loss of either Rb or p53 enhances NE rupture

In order to visualize NE rupture, we used NLS-3xmTurquoise2 (NLS3mTurq, three copies of mTurquoise2 fused to the nuclear localization signal of SV40 large T antigen) as the marker for NE integrity (13). After retroviral transduction of the marker into RPE-1 cells, cells were sorted for Turquoise fluorescence using FACS. The NLS3mTurq marker was stably expressed in the FACS-sorted RPE-1 cells and showed nuclear localization. To determine the effect of Rb or p53 deficiency, RPE-1 NLS3mTurq cells were infected with empty vector (vector), Rb shRNA (Rbsh) or p53 shRNA (p53sh) (19, 20), resulting in a significant depletion of Rb or p53 protein (Fig. 1A). Rb or p53 depletion did not significantly change the ploidy of the cell population (Supplementary Fig. S1A).

To evaluate NE rupture, populations of cells were imaged for 24 hours at 5-minute intervals using spinning disk confocal microscopy. Ninety adjacent fields were then computationally stitched together to allow hundreds of cells to be tracked. The two daughter cells from individual cells that divided in early time frames were followed until they had reached the second mitosis. NE rupture was scored based on the reduction of the nuclear Turquoise fluorescence intensity coin-

cident with transient appearance of Turquoise in the cytoplasm (ref. 6; Fig. 1B).

Upon depletion of either Rb or p53, cells showed increased frequency of NE rupture, manifested by the rapid efflux of NLS3mTurq marker from the nucleus into the cytoplasm (Fig. 1B). Fifty daughter cells from 25 dividing cells in each cell line were examined. The percentage of cells undergoing at least one NE rupture event was 21% ± 3% and 29 ± 3% for the Rb- and p53-depleted cells, respectively (Fig. 1C). This frequency of NE rupture was significantly increased compared to cells infected with the empty vector (Fig. 1C), which showed NE rupture at 3% consistent with a previous analysis of NE rupture of RPE-1 cells (13).

In all cases of NE rupture, the nuclear localization of NLS3mTurq was gradually reestablished, usually within half an hour (Fig. 1D), indicating that the ruptured NE had been re-sealed and nuclear import was functional. The rate at which the nuclear localization of NLS3mTurq was restored was consistent with a previous report (6), and there was no difference between the cells with or without Rb or p53 ( $P = 0.98$ , Kolmogorov-Smirnov test). Strikingly, some Rb- or p53-deficient cells underwent 8 or 9 NE rupture events in one cell cycle (Fig. 1E). All cells with an NE rupture event appeared to survive and progressed through the next mitosis, indicating that a prior NE rupture event does not inhibit cell division.

To confirm the role of Rb and p53 in preventing NE rupture, we used CRISPR/Cas9 to generate Rb and p53 knockout RPE-1 cells. RPE-1 NLS3mTurq cells were nucleofected with plasmids containing mCherry-Cas9 and sgRNA targeting the Rb or p53 locus (Fig. 2A), and mCherry-positive cells were collected in bulk. Western blot showed efficient knockout of Rb and p53 (Fig. 2B), and FACS analysis showed no significant difference in ploidy after Rb or p53 knockout (Supplementary Fig. S1B). Similar to cells with Rb and p53 depletion by shRNA, Rb and p53 knockout cell populations also showed significantly increased frequency of NE rupture compared to the empty vector control cells, reinforcing

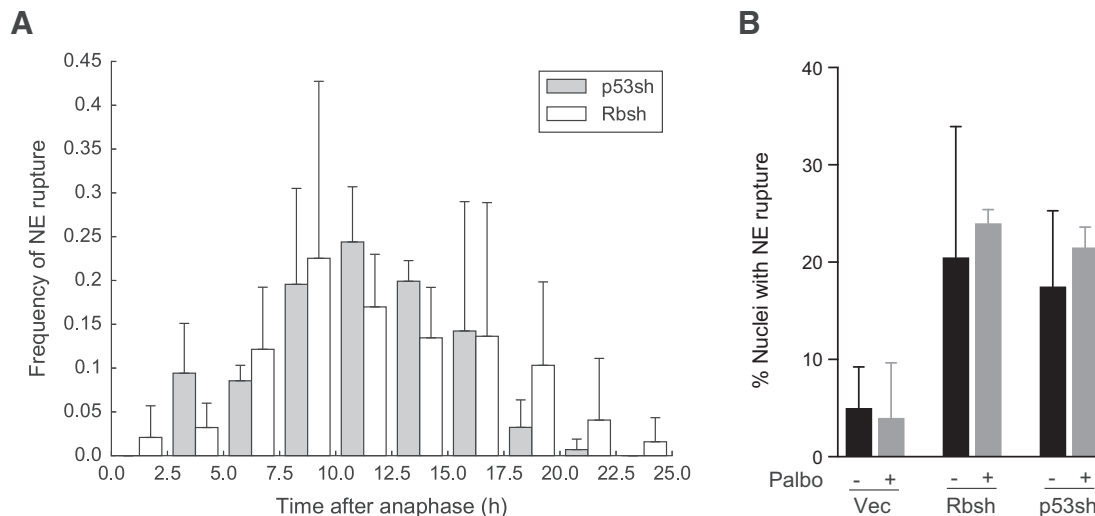


**Figure 3.**

NE rupture can take place in G<sub>1</sub>. **A**, Frequency of NE rupture at the indicated time intervals after anaphase in Rb- or p53-depleted cells. Error bars indicate SD of three separate experiments. All NE rupture events in all analyzed cells are included. **B**, Quantification of the percentage of nuclei with NE rupture in cells treated with or without 1 μmol/L Palbociclib (Palbo). Error bars indicate SD and are derived from two separate experiments.

the idea that both Rb and p53 are important in protecting cells against NE rupture (Fig. 2C). To determine whether the combined loss of p53 and Rb further exacerbates NE rupture, we knocked down Rb with shRNA in p53 knockout cells (Fig. 2D). After Rb depletion, p53 knockout cells had a significantly increased frequency of NE rupture, indicating that Rb and p53 function in different pathways that prevent NE rupture (Fig. 2E).

#### NE rupture does not require progression through S phase

We analyzed the timing of NE rupture after mitosis of the Rb- and p53-depleted cells. In both cases, NE rupture frequency gradually increased after mitosis and peaked at around 10 hours after mitosis (Fig. 3A). The data indicate that NE rupture is less likely to occur immediately after mitosis and becomes more frequent as cells go through G<sub>1</sub> and enter S phase.

To understand whether G<sub>1</sub>-S transition has a role in promoting NE rupture, we treated the cells with the CDK4/6 inhibitor Palbociclib at the beginning of the imaging sessions. As expected, 1  $\mu$ mol/L palbociclib treatment completely blocked the cells to G<sub>1</sub> in the case of empty vector and p53-depleted cells (Supplementary Fig. S1C). In Rb-depleted cells, palbociclib treatment only halved the number of cells in S phase (Supplementary Fig. S1C), probably because the main pathway by which CDK4/6 promote G<sub>1</sub>-S transition is by phosphorylating and inactivating Rb. However, treatment with Palbociclib did not reduce the occurrences of NE rupture in Rb- and p53-depleted cells (Fig. 3B). These data indicate that NE rupture can take place in G<sub>1</sub> and that the effect of Rb and p53 knockdown is unlikely to be directly related to a change in G<sub>1</sub>-S transition in these cells.

#### Effects of Rb and p53 loss on expression of NE components and regulatory proteins

In order to understand how loss of Rb and p53 affected NE integrity, we performed immunoblots to examine lamins and lamin-associated proteins that were previously implicated in NE rupture (4, 6, 8). To avoid any off-target effects of shRNA and CRISPR/Cas9 editing, we only considered those proteins that showed similarly significant difference both in cells with shRNA-mediated knockdown and CRISPR/Cas9 knockout. There was no significant difference in lamin A/C (LMNA/C) or lamin B1 (LMNB1) expression upon loss of Rb or p53 (Fig. 4A). We also did not observe any significant changes in SUN1 or SUN2 expression level upon Rb or p53 depletion (Fig. 4A).

Since increased levels of LAP2 (TMPO) can suppress NE rupture in cells with chromatin bridges (13), we also monitored the expression of LAP2 in Rb- and p53-depleted cells. There was no indication of LAP2 deficiency in the cells with elevated NE rupture. On the contrary, both splice variant of LAP2, LAP2 $\alpha$  and LAP2 $\beta$ , were slightly elevated in Rb- and p53-depleted cells (Fig. 4A).

We also examined the level of FMN2, because of its role in maintaining NE integrity during migration through confined spaces (17) and because FMN2 is downregulated by the Rb-controlled factor E2F1 (21). However, immunoblotting did not indicate significant changes in the FMN2 protein level upon Rb or p53 depletion (Fig. 4B).

Finally, we looked at the expression of two ESCRT-III complex proteins, CHMP2A and CHMP4B, because of their role in repairing NE rupture after cells migrate through restrictions (10, 11). Also in this case, there was no significant decrease in

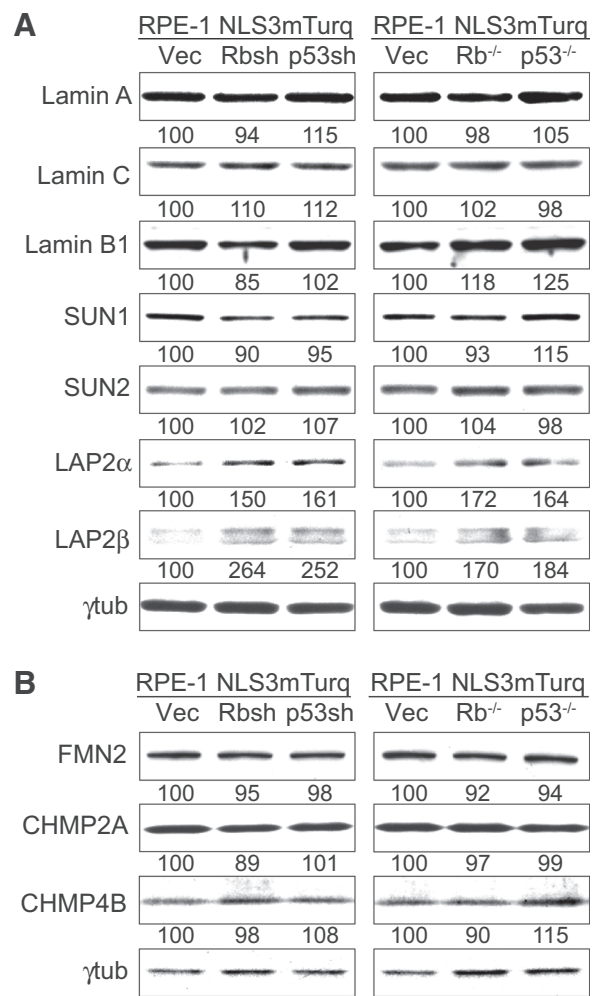


**Figure 4.**

Examination of NE protein expression after loss of Rb or p53. **A**, Immunoblotting of lamins or lamin associated proteins with  $\gamma$ -tubulin as the loading control. The numbers below each band represent the band intensity normalized to the empty vector controls. **B**, Immunoblotting of FMN2, and the ESCRT-III proteins CHMP2A and CHMP4B with  $\gamma$ -tubulin as the loading control.

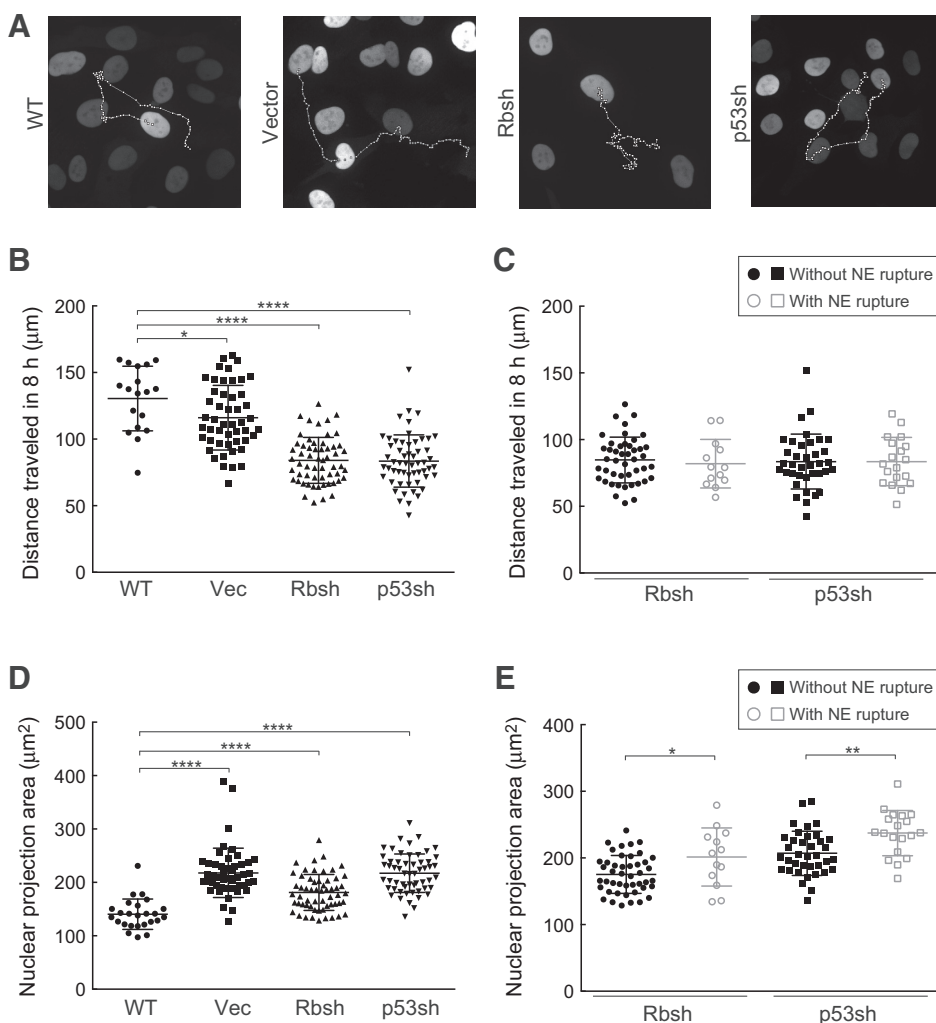
the expression level of these two proteins upon Rb or p53 depletion (Fig. 4B).

#### Effects of Rb and p53 loss on cell motility and nuclear projection area

It has been shown that Rb or p53 depletion can increase cell motility (22–24). Given that both the actin cytoskeleton and the stiffness of the cell substratum can affect NE rupture (7, 9), we tested whether the enhanced NE rupture in p53- and Rb-depleted cells could be ascribed to a change in cell motility. We manually tracked the movement of cells (Fig. 5A) and found a significant decrease, rather than an increase, in cell motility upon loss of Rb or p53 (Fig. 5B). We also compared the cells with and without NE rupture and found that there is no difference in their migration behavior (Fig. 5C).

Finally, we sought to determine the effect of Rb and p53 loss on the nuclear projection area. An increase in the nuclear

Yang et al.

**Figure 5.**

Migration rate and nuclear projection area of cells with NE rupture. **A**, Examples of cell tracking over an 8-hour time period. **B** and **C**, Quantification of the distance that individual cells traveled in 8 hours. The error bars indicate SDs. Statistical significance analysis by Student *t* test (\*,  $P < 0.05$ ; \*\*\*\*,  $P < 0.0001$ ). One-way ANOVA in (**B**),  $P < 0.0001$ . **D** and **E**, Quantification of the nuclear projection area of individual cells. The error bars indicate SDs. Statistical significance analysis by the Student *t*-test (\*,  $P < 0.05$ ; \*\*,  $P < 0.01$ ; \*\*\*\*,  $P < 0.0001$ ). Where no stars are given, there was no significant difference. One-way ANOVA in (**D**),  $P < 0.0001$ .

projection area could be an indication of increased nuclear size or a flattened nucleus, which is correlated with an increase in the mechanical stress. Unexpectedly, we found that there was a significant increase in nuclear projection area upon infection of the cells with the shRNAs vectors (Fig. 5D). However, this effect was also observed with the vector not expressing shRNAs, indicating that it is not relevant to the increased NE rupture upon p53 or Rb knockdown.

We also compared the nuclear projection area of cells that did or did not undergo NE rupture, using the Rb- or p53-depleted cells. Interestingly, those cells undergoing NE rupture displayed slightly larger nuclear projection area (Fig. 5E).

## Discussion

Given that the majority of human cancers are deficient in either the Rb or p53 pathway, our finding that both Rb and p53 prevent NE rupture has significant implications. Indeed, in each of the three cancer cell lines in which NE rupture has so far been documented, HeLa, U2OS, and SJSa (6), either Rb or p53 pathway has been shown to be defective. In HeLa cells, the tumor suppressor p53 is undetectable owing to the expression of HPV E6 (25, 26). In U2OS cells, the *CDKN2A* locus is silenced by DNA

methylation (27), and as a result, Rb is constitutively hyperphosphorylated and inactivated (28). In the case of SJSa, the p53 pathway is inactivated because of the amplification of the *MDM2* gene (29). Therefore, our findings could potentially explain the frequent occurrence of NE rupture in these cancer cell lines.

NE rupture could have an impact on gene regulation, not only because of mislocalized transcription factors, but also due to disruption of the lamin network, which can affect gene regulation (30). Furthermore, NE rupture has been reported to lead to DNA damage (10, 11), potentially resulting from the introduction of cytoplasmic nucleases into the nucleoplasm. In micronuclei as well as in cells experiencing telomere damage, NE rupture can lead to chromothripsis (13, 16, 31, 32). Thus, NE rupture may change the genomic landscape in cancer cells, thereby contributing to carcinogenesis. Because we show that p53- or Rb-deficient cells can undergo several rounds of NE rupture without losing the ability to progress into mitosis, this process could substantially enhance their carcinogenic potential.

We have not been able to identify the mechanism by which Rb or p53 deficiency leads to NE rupture. Expression levels of a number of relevant proteins, including NE components, the ESCRT-III complex, and FMN2, were not overtly changed by the

loss of Rb and p53. Further work on the (ultra) structure of the NE in these cells will be required to define the pathway by which Rb and p53 ensure NE integrity.

Interestingly, we found that the level of LAP2 $\alpha$  and LAP2 $\beta$ , the two splicing variants of LAP2, was slightly increased after Rb depletion. Mouse LAP2 $\alpha$  has been implicated in tethering Rb to A-type lamins, thereby preventing the proteosomal degradation of the protein (33, 34). In addition, in mouse, LAP2 $\beta$  can recruit Germ-cell-less (mGCL) protein to the lamina and repress the activity of the E2F- $\Delta$ DP3 complex, the main target of Rb (35). Furthermore, overexpression of LAP2 is able to suppress the NE rupture phenotype (13). Upon Rb depletion, cells with increased LAP2 may experience a selective advantage and/or there may be a feedback loop that gives rise to higher LAP2 levels when Rb is repressed.

Our data provide a critical link between tumor suppressors and NE integrity. It will therefore be of interest to uncover the detailed mechanism by which tumor suppressors Rb and p53 prevent NE rupture. In addition, it is important to determine whether NE rupture could occur in primary tumors, and if so, whether targeting pathways that maintain NE could induce synthetic lethality in Rb- or p53-deficient cancers.

#### Disclosure of Potential Conflicts of Interest

No potential conflicts of interest were disclosed.

#### Disclaimer

The content of this article is solely the responsibility of the authors and does not necessarily represent the official views of the National Center for Research Resources or the NIH.

#### References

- Hetzer MW. The nuclear envelope. *Cold Spring Harb Perspect Biol* 2010;2:a000539.
- Güttinger S, Laurrell E, Kutay U. Orchestrating nuclear envelope disassembly and reassembly during mitosis. *Nat Rev Mol Cell Biol* 2009;10:178–91.
- Hatch E, Hetzer M. Breaching the nuclear envelope in development and disease. *J Cell Biol* 2014;205:133–41.
- De Vos WH, Houben F, Kamps M, Malhas A, Verheyen F, Cox J, et al. Repetitive disruptions of the nuclear envelope invoke temporary loss of cellular compartmentalization in laminopathies. *Hum Mol Genet* 2011;20:4175–86.
- Porwal M, Cohen S, Snoussi K, Popa-Wagner R, Anderson F, Dugot-Senant N, et al. Parvoviruses cause nuclear envelope breakdown by activating key enzymes of mitosis. *PLoS Pathog* 2013;9:e1003671.
- Vargas JD, Hatch EM, Anderson DJ, Hetzer MW. Transient nuclear envelope rupturing during interphase in human cancer cells. *Nucleus* 2014;3:88–100.
- Hatch EM, Hetzer MW. Nuclear envelope rupture is induced by actin-based nucleus confinement. *J Cell Biol* 2016;215:27–36.
- Chen CY, Chi YH, Mutalif RA, Starost MF, Myers TG, Anderson SA, et al. Accumulation of the inner nuclear envelope protein Sun1 is pathogenic in progeric and dystrophic laminopathies. *Cell* 2012;149:565–77.
- Tamiello C, Kamps MA, van den Wijngaard A, Verstraeten VL, Baaijens FP, Broers JL, et al. Soft substrates normalize nuclear morphology and prevent nuclear rupture in fibroblasts from a laminopathy patient with compound heterozygous LMNA mutations. *Nucleus* 2014;4:61–73.
- Raab M, Gentili M, de Belly H, Thiam HR, Vargas P, Jimenez AJ, et al. ESCRT III repairs nuclear envelope ruptures during cell migration to limit DNA damage and cell death. *Science* 2016;352:359–62.
- Denais CM, Gilbert RM, Isermann P, McGregor AL, Lindert M, Weigel B, et al. Nuclear envelope rupture and repair during cancer cell migration. *Science* 2016;352:353–8.
- Le Berre M, Aubertin J, Piel M. Fine control of nuclear confinement identifies a threshold deformation leading to lamina rupture and induction of specific genes. *Integr Biol* 2012;4:1406–14.
- Maciejowski J, Li Y, Bosco N, Campbell PJ, de Lange T. Chromothripsis and kataegis induced by telomere crisis. *Cell* 2015;163:1641–54.
- Hatch EM, Fischer AH, Deerinck TJ, Hetzer MW. Catastrophic nuclear envelope collapse in cancer cell micronuclei. *Cell* 2013;154:47–60.
- Crasta K, Ganem NJ, Dagher R, Lantermann AB, Ivanova EV, Pan Y, et al. DNA breaks and chromosome pulverization from errors in mitosis. *Nature* 2012;482:53–8.
- Zhang CZ, Spektor A, Cornils H, Francis JM, Jackson EK, Liu S, et al. Chromothripsis from DNA damage in micronuclei. *Nature* 2015;522:179–84.
- Skau CT, Fischer RS, Gurel P, Thiam HR, Tubbs A, Baird MA, et al. FMN2 makes perinuclear actin to protect nuclei during confined migration and promote metastasis. *Cell* 2016;167:1571–85.
- Preibisch S, Saalfeld S, Tomancak P. Globally optimal stitching of tiled 3D microscopic image acquisitions. *Bioinformatics* 2009;25:1463–5.
- Masutomi K, Yu EY, Khurts S, Ben-Porath I, Currier JL, Metz GB, et al. Telomerase maintains telomere structure in normal human cells. *Cell* 2003;114:241–53.
- Boehm JS, Hession MT, Bulmer SE, Hahn WC. Transformation of human and murine fibroblasts without viral oncoproteins. *Mol Cell Biol* 2005;25:6464–74.
- Yamada K, Ono M, Perkins ND, Rocha S, Lamond AI. Identification and functional characterization of FMN2, a regulator of the cyclin-dependent kinase inhibitor p21. *Mol Cell* 2013;49:922–33.
- Gadea G, de Toledo M, Anguille C, Roux P. Loss of p53 promotes RhoA-ROCK-dependent cell migration and invasion in 3D matrices. *J Cell Biol* 2007;178:23–30.
- Kim KJ, Godarova A, Seedle K, Kim MH, Ince TA, Wells SI, et al. Rb suppresses collective invasion, circulation and metastasis of breast cancer

#### Authors' Contributions

**Conception and design:** Z. Yang, J. Maciejowski, T. de Lange  
**Development of methodology:** J. Maciejowski, T. de Lange  
**Acquisition of data (provided animals, acquired and managed patients, provided facilities, etc.):** Z. Yang  
**Analysis and interpretation of data (e.g., statistical analysis, biostatistics, computational analysis):** Z. Yang  
**Writing, review, and/or revision of the manuscript:** Z. Yang, J. Maciejowski, T. de Lange  
**Administrative, technical, or material support (i.e., reporting or organizing data, constructing databases):** Z. Yang  
**Study supervision:** T. de Lange

#### Acknowledgments

The authors thank members of the de Lange lab for comments on this article. We also thank K. Thomas, T. Tao, and A. North of the RU Bio-imaging Core Facility for their expert assistance with microscopy.

#### Grant Support

J. Maciejowski is supported by a grant from the NIH (K99CA212290). Research reported in this publication was supported by an OIA to T. de Lange from the NCI (R35CA210036) and grants to T. de Lange from the BCRF and the Starr Foundation Cancer Consortium (19-A9-047). T. de Lange is an American Cancer Society Rose Zarucki Trust Research Professor. Bio-Imaging Center at RU is supported by a grant (S10RR031855) from the National Center For Research Resources to the Bio-Imaging Center at RU.

The costs of publication of this article were defrayed in part by the payment of page charges. This article must therefore be hereby marked *advertisement* in accordance with 18 U.S.C. Section 1734 solely to indicate this fact.

Received February 13, 2017; revised July 5, 2017; accepted August 11, 2017; published OnlineFirst August 15, 2017.

Yang et al.

- cells in CD44-dependent manner. Mehta K, editor. *PLoS One* 2013;8:e80590.
24. Hwang CI, Matoso A, Corney DC, Flesken-Nikitin A, Körner S, Wang W, et al. Wild-type p53 controls cell motility and invasion by dual regulation of MET expression. *Proc Natl Acad Sci* 2011;108:14240–5.
  25. Matlashewski G, Banks L, Pim D, Crawford L. Analysis of human p53 proteins and mRNA levels in normal and transformed cells. *Eur J Biochem* 1986;154:665–72.
  26. Scheffner M, Münger K, Byrne JC, Howley PM. The state of the p53 and retinoblastoma genes in human cervical carcinoma cell lines. *Proc Natl Acad Sci* 1991;88:5523–7.
  27. Park YB, Park MJ, Kimura K, Shimizu K, Lee SH, Yokota J. Alterations in the INK4a/ARF locus and their effects on the growth of human osteosarcoma cell lines. *Cancer Genet Cytogenet* 2002;133:105–11.
  28. Broceño C, Wilkie S, Mitnacht S. RB activation defect in tumor cell lines. *Proc Natl Acad Sci* 2002;99:14200–5.
  29. Oliner JD, Kinzler KW, Meltzer PS, George DL, Vogelstein B. Amplification of a gene encoding a p53-associated protein in human sarcomas. *Nature* 1992;358:80–3.
  30. Dechat T, Pfliegerhaer K, Sengupta K, Shimi T, Shumaker DK, Solimando L, et al. Nuclear lamins: Major factors in the structural organization and function of the nucleus and chromatin. *Genes Dev* 2008;22:832–53.
  31. Stephens PJ, Greenman CD, Fu B, Yang F, Bignell GR, Mudie LJ, et al. Massive genomic rearrangement acquired in a single catastrophic event during cancer development. *Cell* 2011;144:27–40.
  32. Nik-Zainal S, Alexandrov LB, Wedge DC, Van Loo P, Greenman CD, Raine K, et al. Mutational processes molding the genomes of 21 breast cancers. *Cell* 2012;149:979–93.
  33. Johnson BR, Nitta RT, Frock RL, Mounkes L, Barbie DA, Stewart CL, et al. A-type lamins regulate retinoblastoma protein function by promoting sub-nuclear localization and preventing proteasomal degradation. *Proc Natl Acad Sci* 2004;101:9677–82.
  34. Nitta RT, Jameson SA, Kudlow BA, Conlan LA, Kennedy BK. Stabilization of the retinoblastoma protein by A-type nuclear lamins is required for INK4A-mediated cell cycle arrest. *Mol Cell Biol* 2006;26:5360–72.
  35. Nili E, Cojocaru GS, Kalma Y, Ginsberg D, Copeland NG, Gilbert DJ, et al. Nuclear membrane protein LAP2 $\beta$  mediates transcriptional repression alone and together with its binding partner GCL (germ-cell-less). *J Cell Sci* 2001;114:3297–307.

# Molecular Cancer Research

## Nuclear Envelope Rupture Is Enhanced by Loss of p53 or Rb

Zhe Yang, John Maciejowski and Titia de Lange

*Mol Cancer Res* 2017;15:1579-1586. Published OnlineFirst August 15, 2017.

**Updated version** Access the most recent version of this article at:  
doi:[10.1158/1541-7786.MCR-17-0084](https://doi.org/10.1158/1541-7786.MCR-17-0084)

**Supplementary Material** Access the most recent supplemental material at:  
<http://mcr.aacrjournals.org/content/suppl/2017/11/14/1541-7786.MCR-17-0084.DC1>

**Cited articles** This article cites 35 articles, 14 of which you can access for free at:  
<http://mcr.aacrjournals.org/content/15/11/1579.full#ref-list-1>

**E-mail alerts** [Sign up to receive free email-alerts](#) related to this article or journal.

**Reprints and Subscriptions** To order reprints of this article or to subscribe to the journal, contact the AACR Publications Department at [pubs@aacr.org](mailto:pubs@aacr.org).

**Permissions** To request permission to re-use all or part of this article, use this link  
<http://mcr.aacrjournals.org/content/15/11/1579>.  
Click on "Request Permissions" which will take you to the Copyright Clearance Center's (CCC) Rightslink site.

**Supplementary Figure 1. FACS analysis of cells with Rb or p53 depletion.**

(A and B) FACS analysis of Propidium iodide (PI) staining in indicated cell lines to quantify the percentage of hyperploid cells. Quantification of hyperploid cells is based on cells with more than 4n DNA content.

(C) FACS analysis of BrdU and PI staining in indicated cell lines treated with or without 1  $\mu$ M Palbociclib (Palbo) to quantify the percentage of cells in S phase. Quantification of S phase cells is based on cells that are BrdU positive.

Supplementary Figure 1. Yang et al.

